Organic LETTERS

Letter

pubs.acs.org/OrgLett

Four New Polycyclic Meroterpenoids from *Ganoderma cochlear*

Xing-Rong Peng,[†,‡] Jie-Qing Liu,[†] Luo-Sheng Wan,[†] Xiao-Nian Li,[†] Yu-Xin Yan,[†] and Ming-Hua Qiu*[,†,‡]

[†]Key Laboratory of Phytochemistry and Plant Resources in West China, Kunming Institute of Botany, Chinese Academy of Sciences, Kunming 650201, People's Republic of China

[‡]Graduate University of the Chinese Academy of Sciences, Beijing 100049, People's Republic of China

Supporting Information

ABSTRACT: Four pairs of new polycyclic-meroterpenoid enantiomers, ganocins A–C (**1**–**3**) possessing a spiro[4,5]decane ring system, along with ganocin D (**4**) with an eight-membered ring, were isolated from the fruiting bodies of *Ganoderma cochlear*. Their structures were determined by spectroscopic data and X-ray diffraction crystallography. Their anti-AChE activities were evaluated, and a possible biogenetic pathway was also proposed.

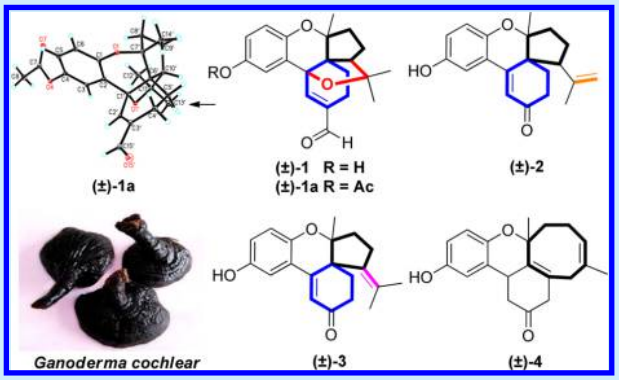

The genus *Ganoderma* (Ganodermataceae) is a basidiomycete white rot fungus mainly distributed in tropical and subtropical areas of Asia. The fungus has been used as a folk medicine to treat and prevent various diseases for centuries, particularly in China, Japan, and Korea.[1] Most of the phytochemical and pharmacological investigations have focused on the ganoderma triterpeniods and polysaccharides.[2] Our group has been interested in the bioactive constituents of *Ganoderma*[3] and was the first to report triterpenoids and the liver-protective activities of *G. cochlear*.[4] However, several phenolic meroterpenoids including ganomycins A and B,[5] fornicins A–C,[6] ganomycin I,[7] and (±)-lingzhiol with a rotated door structure[8] from *Ganoderma* were reported, which attracts our attention.

Acetylcholinesterase (AChE), mainly present in the central nervous system (CNS), catalyzes the hydrolysis of neurotransmitter acetylcholine to choline.[9] This enzyme is related to neurological diseases, such as Alzheimer's disease (AD) and epilepsia.[10] Research has directly demonstrated that *Ganoderma* can enhance memory and protect the nervous system by inhibiting AChE activity.[11] Some natural AChE inhibitors (magnolol and ferulic acid) have a phenolic substructure,[12] suggesting that ganoderma meroterpenoids with the phenolic structure may also show anti-AChE activity.

Thus, we studied the total phenolic parts of *G. cochlear*, and four unprecedented polycyclic meroterpenoids, ganocins A–C (**1**–**3**) possessing a spiro[4,5]decane substructure, and ganocin D (**4**), with an eight-membered carbon ring, were isolated. Herein, we report the structural elucidation including absolute configuration analysis, a biogenetic pathway, and bioactive evaluation of **1**–**4**.

The molecular formula of ganocin A (**1**) was assigned as $C_{21}H_{24}O_4$ by HREIMS ([M]$^+$, m/z 340.1669; calcd 340.1679)

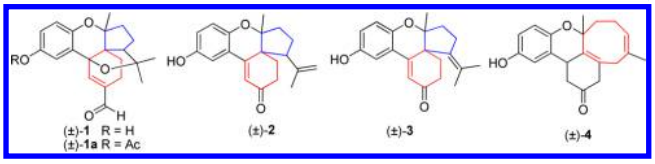

with ten degrees of unsaturation. Its IR spectrum showed the presence of an aldehyde group (2962 and 1758 cm^{-1}). The ^{13}C NMR spectrum (Table 1) exhibited 21 carbon resonances, corresponding to three methyls, four methylenes, five methines (four aromatic/olefinic methines), eight quaternary carbons (one tetrasubstituted carbon, one carbonyl group, one oxygenated quaternary carbon, and four aromatic/olefinic quaternary carbons), and one aldehyde carbon. The ^{1}H NMR spectrum (Table 1) showed three typical aromatic signals at δ 7.01 (d, J = 2.4 Hz), 6.66 (dd, J = 2.4 and 9.0 Hz), and 6.64 (d, J = 9.0 Hz), suggesting the presence of a 1,2,4-trisubstituted dihydroxylbenzene substructure (part A in Figure 1), which was similar to that of fornicin C, a meroterpenoid with a 15 carbon side chain.[6]

Similarly, except for the phenol group (part A), the remaining 15 carbons of **1** were representative of four rings based on its 1D-NMR and the degree of unsaturation.

In the ^{13}C NMR spectrum of **1**, three low-field carbon signals at δ 150.6 (d), δ 139.2 (s), and δ 193.8 (d) were attributed to an α,β-unsaturated aldehyde group (C-2′/C-3′/C-15′), based on the HMBC correlations (Figure 1) of H-2′ with C-2, C-3′, and C-15′. Meanwhile, the HMBC correlations of H-2′ and H-3 with an oxyquaternary carbon (δ 78.1) indicated that the oxyquaternary carbon was located at C-1′. Moreover, the

Received: August 7, 2014
Published: September 5, 2014

dx.doi.org/10.1021/ol5023189 | *Org. Lett.* 2014, 16, 5262–5265

Table 1. ^{1}H and ^{13}C NMR Data for Compounds 1−4 (J in Hz)

	1[b]		2[a]		3[a]		4[a]	
	δ_H	δ_C	δ_H	δ_C	δ_H	δ_C	δ_H	δ_C
1		146.5 (s)		148.4 (s)		149.7 (s)		146.9 (s)
2		129.9 (s)		120.4 (s)		123.4 (s)		122.3 (s)
3	7.01 d (7.4)	113.4 (d)	7.65, d (3.0)	109.9 (d)	7.66, d (3.0)	111.4 (d)	7.14, d (2.4)	109.0 (d)
4		151.2 (s)		151.7 (s)		152.6 (s)		152.3 (s)
5	6.64, m	116.1 (d)	7.20, dd (3.0, 9.0)	121.9 (d)	7.16, dd (3.0, 9.0)	122.1 (d)	7.03, dd (2.4, 9.0)	115.8 (d)
6	6.64, m	119.5 (d)	6.93, d (9.0)	119.4 (d)	6.91, d (9.0)	118.9 (d)	6.97, d (9.0)	116.1 (d)
1′		78.1 (s)		152.6 (s)		154.5 (s)	3.82, t	46.0 (d)
2′	6.62, m	150.6 (d)	6.94, s	120.9 (d)	6.99, s	122.5 (d)	2.29, m	27.4 (t)
3′		139.2 (s)		198.0 (s)		198.8 (s)		212.0 (s)
4′	2.37, m; 2.18, m	19.1 (t)	2.78, m; 2.55, m	33.6 (t)	2.59, m; 2.49, m	34.6 (t)	2.25, m	24.8 (t)
5′	2.07, m; 1.66, m	30.8 (t)	1.86, m; 1.57, m	33.9 (t)	1.84, m; 1.66, m	30.9 (t)		127.7 (s)
6′		60.7 (s)		51.3 (s)		52.2 (s)		133.8 (s)
7′		88.7 (s)		88.5 (s)		90.6 (s)		80.1 (s)
8′	2.07, m; 1.57, m	39.5 (t)	2.10, m; 1.91, m	37.7 (t)	2.62, m; 2.30, m	28.5 (t)	2.35, m; 1.78, m	48.4 (t)
9′	1.69, m	24.0 (t)	2.23, m; 1.89, m	28.2 (t)	2.05, m; 1.85, m	34.5 (t)	2.49, m; 2.33, m	37.5 (t)
10′	2.39, m	62.0 (d)	3.11, t	53.0 (d)		134.5 (s)	5.06, m	133.8 (d)
11′		84.7 (s)		145.8 (s)		126.6 (s)		131.2 (s)
12′	1.17, s	25.8 (q)	1.46, s	22.5 (q)	1.53, s	18.8 (q)	1.67, s	27.5 (q)
13′	1.30, s	32.5 (q)	4.79, s; 4.70, s	114.3 (t)	1.34, s	23.1 (q)	2.60, br s	36.7 (t)
14′	1.42, s	23.9 (q)	1.23, s	18.9 (q)	1.21, s	17.4 (q)	1.54, s	24.8 (q)
15′	9.40, s	193.8 (d)						

[a]Measured in C_5D_5N. [b]Measured in $CDCl_3$. 1D NMR spectra (δ) were measured at 400 (100) MHz for **1** and at 600 (150) MHz for **2**−**4**. The assignments were based on $^{1}H-^{1}H$ COSY, ROESY, HSQC, and HMBC experiments.

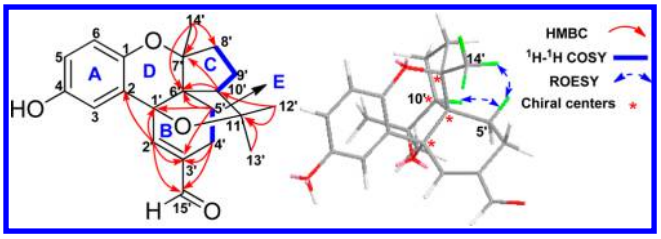

Figure 1. Key HMBC, $^{1}H-^{1}H$ COSY, and ROESY correlations of (±)-**1**.

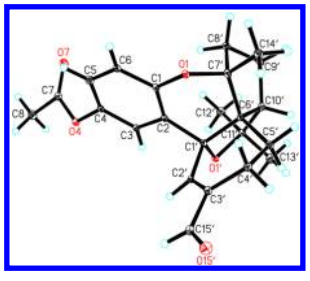

Figure 2. X-ray crystallographic structure of **1a**.

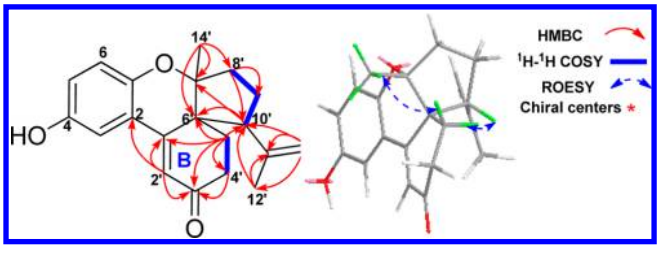

Figure 3. Key HMBC, $^{1}H-^{1}H$ COSY, and ROESY correlations of (±)-**2**.

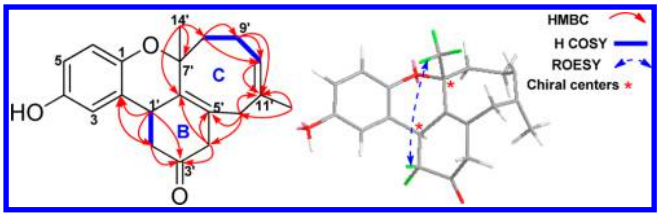

Figure 4. Key HMBC, $^{1}H-^{1}H$ COSY, and ROESY correlations of (±)-**4**.

observed HMBC correlations from H-2′, H_2-4′, and H_2-5′ to C-3′ and a quaternary carbon (δ 60.7), together with the $^{1}H-^{1}H$ COSY correlations of H_2-4′/H_2-5′, confirmed that C-1′ is connected with C-6′ (δ 60.7) to form a cyclohex-1-ene-1-carbaldehyde substructure (B ring) in **1**.

Subsequently, the presence of CH_2-8′/CH_2-9′/CH-10′ moiety was deduced by the $^{1}H-^{1}H$ COSY correlations. In the HMBC spectrum of **1**, H_2-8′, H_2-5′, and H_3-14′ (δ 1.42, s) showed the HMBC correlations with an oxyquaternary carbon (δ 88.7), which indicated that C-7′ was the oxyquaternary carbon. Meanwhile, only H-10′ showed the HMBC correlations with another oxyquaternary carbon (δ 84.7) and two methyls (δ 25.8, δ 32.5), suggesting a 2-oxyisopropyl group was located at C-10′. Importantly, the key HMBC correlations of H_2-8′ and H-10′ with C-6′ and C-7′ were observed. Thus, we unambiguously deduced that a five-membered ring (part C) and B ring formed a spiro[4,5]decane ring system.

Apart from the above-mentioned two rings, another two rings were finally determined as 1,7′-epoxy and 1′,11′-epoxy rings, based on its formula weight and degrees of unsaturation (Figure 1).

The ROESY correlations of H_3-14′/H_2-5′/H-10′ indicated that CH_3-14′, CH_2-5′, and H-10′ were on the same face. Furthermore, the single-crystal X-ray diffraction of acetylated

dx.doi.org/10.1021/ol5023189 | Org. Lett. 2014, 16, 5262−5265

Scheme 1. A Plausible Biogenetic Pathway for 1−4

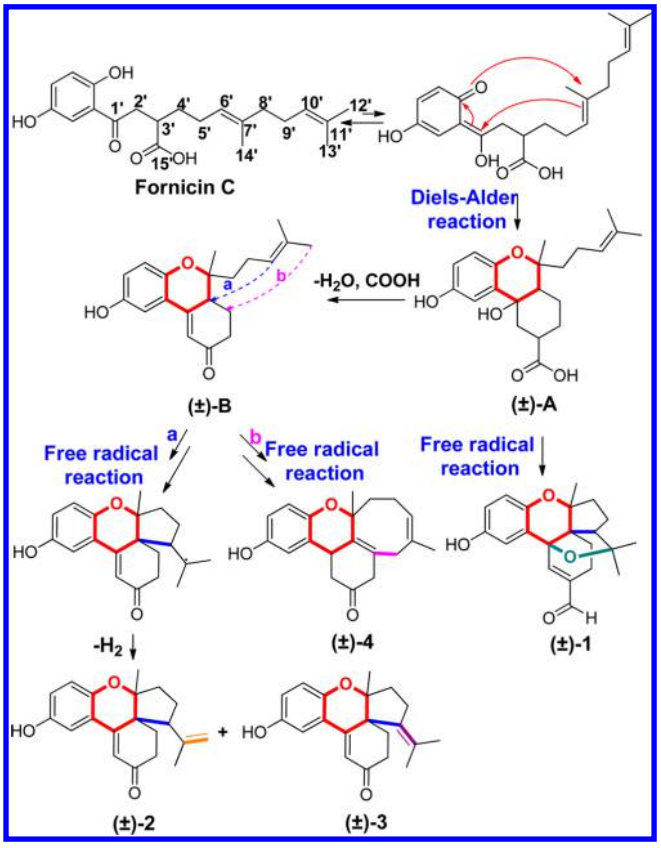

derivative of **1** (Figure 2) showed that acetyl ganocin D (**1a**) was a pair of enantiomers. Thus, the single-crystal X-ray diffraction experiment of **1a** performed by using Cu Kα radiation confirmed **1a** as 1′*R*,6′*R*,7′*R*,10′*R* and 1′*S*,6′*S*,7′*S*,10′*S*.

Ganocin B (**2**) was obtained as a yellow powder with a molecular ion peak at *m*/*z* 310.1564 $[M]^+$ in HREIMS, coinciding with the molecular formula $C_{20}H_{22}O_3$. A comparison of 1D NMR spectroscopic data between **2** and **1** showed that **2** also had a 1,2,4-trisubstituted dihydroxylbenzene substructure and a spiro[4,5]decane ring system, which was further supported by its 2D NMR spectra (Figure 3). However, the ^{13}C NMR spectrum of **2** showed 20 carbons, with one less carbon than **1**. Obviously, in the 1D NMR spectra of **2**, an α,β-unsaturated ketone (δ 152.6; δ 120.9, and δ 198.0) was observed, instead of the aldehyde group signal in **1**. We speculated that the B ring of **2** was a cyclohexenone moiety and the α,β-unsaturated ketone was attributable to C-1′, C-2′, and C-3′. This was confirmed by the HMBC correlations of the olefinic proton (δ 6.94, s) with C-2, the olefinic quaternary carbon (δ 152.6), and the carbonyl group and C-6′; of H-3 and H_2-5′ with the olefinic quaternary carbon; and of H_2-4′ and H_2-5′ with the carbonyl group and C-6′. Additionally, a terminal double bond (δ 4.79, s, δ 4.70, s; δ 114.3 and δ 145.8) was assigned to C-11′ and C-13′ by the HMBC correlations of the olefinic protons at δ 4.79 (s) and δ 4.70 (s) with CH_3-12′ (δ 22.5) and C-10′ (δ 53.0). Thus, the planar structure of **2** was established.

The ROESY correlations of H_3-14/H_2-5/H-10′ suggested that CH_3-14′, C-6′, and C-10′ had the same relative configuration (Figure 3). Its optical rotation value ($[\alpha]^{20}_D$ +1.8) indicated a racemic nature, and the subsequent chiral resolution of **2** by HPLC afforded the anticipated enantiomers, **2a** and **2b**, which were opposite in terms of their CD curve and $[\alpha]_D$ spectra ($[\alpha]^{20}_D$ +117.9 and $[\alpha]^{20}_D$ −104.6) (see Supporting Information (SI)). Therefore, **2** was deduced to be 6′*R*,7′*R*,10′*R* and 6′*S*,7′*S*,10′*S*.

Ganocin C (**3**) has the same molecular formula $C_{20}H_{22}O_3$ established by the $[M]^+$ ion peak at *m*/*z* 310.1566 in the HREIMS as compound **2**. The 1D NMR spectroscopic data of **3** were similar to those of **2**, except that a methyl (δ 23.1, C-13′) and two olefinic quaternary carbons (δ 134.5, C-10′ and δ 126.6, C-11′) in **3** replaced the terminal double bond and a methine in **2**, which was confirmed by the HMBC correlations of H_3-12′ (δ 1.54, s) and H_3-13′ (δ 1.34, s) with two olefinic quaternary carbons and of H_2-5′, H_2-8′ and H_2-9′ with the olefinic quaternary carbon (δ 134.5). Its ROESY spectrum showed an interaction between H_2-5′ and H_3-14′, suggesting that CH_3-14′ and C-5′ were ipsilateral. Its optical rotation value ($[\alpha]^{20}_D$ −0.7) indicated that **3** could be a pair of enantiomers, which was supported by HPLC analysis on an analytical chiral column, showing two peaks (see SI). Due to only two chiral centers in **3**, C-6′ and C-7′ were assigned as *R*,*R* and *S*,*S*.

The molecular formula of ganocin D (**4**) assigned as $C_{20}H_{22}O_3$ by its ion peak at *m*/*z* 310.1573 $[M]^+$ (calcd 310.1569) in the HREIMS spectrum was also the same as that for compound **3**. However, the chemical shift of the carbonyl carbon was shifted low-field to 212.0 ppm, suggesting the absence of the double bond ($\Delta^{1,2}$) in **4**. This was confirmed by the HMBC correlations (Figure 4) of H-1′ (δ 3.82, t), H_2-2′ (δ 2.29, m) with C-1 and C-3′ and of H-3 with C-1′ (Figure 4). Additionally, the observed HMBC correlations of H-1′ and H_2-4′, with two olefinic quaternary carbons (δ 127.7 and δ 133.8), suggested the existence of C-5′═C-6′, which indicated that the quaternary carbon (C-6′) in **3** was replaced by an olefinic quaternary carbon in **4**. From this, we speculated that its C ring was different from that of **3**.

On the basis of the HMBC correlations of methylene protons (δ 2.35, m; δ 1.78, m), H-1′ and H_3-14′ with C-7′ (δ 80.1), the methylene was assigned to C-8′. The $^1H-^1H$ COSY spectrum deduced the presence of the $-CH_2-CH_2-CH=$ moiety (C-8′/C-9′/C-10′), of which H-10′ showed an HMBC correlation with C-11′, CH_3-12′, and a methylene (δ 36.7). This indicated that the methylene in **4** replaced CH_3-13′ in **3**. Meanwhile, H_2-13′ showed the HMBC correlations with C-4′, C-5′, and C-6′, which confirmed that the C ring of **4** was an eight-membered ring. Thus, the planar structure of **4** was determined as shown in Figure 4.

The ROESY correlations of H_2-2′/H_3-14′ indicated that the relative configurations of H-1′ and CH_3-14′ were reverse (Figure 4). On the basis of its optical rotation value and the chiral HPLC analysis result (see SI), **4** was finally established to be 1′*R*,6′*R* and 1′*S*,6′*S*.

Ganocins A−C (**1**−**3**) possessing a spiro[4,5]decane substructure and ganocin D (**4**) with an eight-membered ring were established to be polycyclic enantiomers. Compared to fornicins A−C, all of them have a 1,2,4-trisubstituted dihydroxylbenzene moiety. We deduced that the B and D rings of **1**−**4** were formed by the hetero-Diels−Alder reaction of fornicin C. Meanwhile, the prenylated side chain of fornicins A−C could provide appropriate conditions for a free radical reaction. The dienophile may be directed away from diene (*exo* approach) or toward the diene (*endo* approach) to produce a pair of enantiomers,[13] which also would biosynthetically explain the racemic nature of compounds **1**−**4**. The C ring was

dx.doi.org/10.1021/ol5023189 | *Org. Lett.* 2014, 16, 5262−5265

subsequently derived from the further free radical reactions. Thus, a plausible biogenetic pathway for **1**–**4** was proposed (Scheme 1).

Research showed that the extracts of *Ganoderma* can decrease AChE to protect the CNS and improve memory.[11] In the present study, the evaluation of anti-AChE effects showed that compound **4** had weak anti-AChE activity with an inhibition of 32% (50 μM). Nevertheless, other compounds are inactive. Compared to natural phenolic AChE inhibitors with a big conjugated system (flavonoids and anthraquinones),[12] compounds **1**–**4** only had a benzene ring. We deduced that their low conjugation system and coplanarity affected their anti-AChE activity.

■ ASSOCIATED CONTENT

Supporting Information

1D and 2D NMR spectra of **1**–**4**, the data for single-crystal X-ray diffraction of **1a** (CIF), $[\alpha]_D$ spectra and CD spectra for **2a** and **2b**, and in vitro anti-AChE activity of **1**–**4**, together with experimental details. This material is available free of charge via the Internet at http://pubs.acs.org.

■ AUTHOR INFORMATION

Corresponding Author

*E-mail: mhchiu@mail.kib.ac.cn.

Notes

The authors declare no competing financial interest.

■ ACKNOWLEDGMENTS

The project was financially supported by the General Program of NSFC (No. 81172940) and Knowledge Innovation Program of the CAS (Grant No. KSZD-EW-Z-004-01, KSCX2-YW-R-194), as well as the Foundation of State Key Laboratory of Phytochemistry and Plant Resources in West China (P2010-ZZ14). The authors were particularly grateful to Mr. Jonathan Teichroew from the Kunming Institute of Botany, Chinese Academy of Sciences, for assistance with English.

■ REFERENCES

(1) (a) Reishi, K. J. *Ancient Herb for Modern Times*; Sylvan Press: London, 1992. (b) Lin, Z. B., Ed. *Modern Research on Lingzhi*, 2nd ed.; Beijing Medical University Press: Beijing, 2001.

(2) (a) Zhou, Y. Q.; Yang, X. T.; Yang, Q. Y. *Food Rev. Int.* **2006**, *22*, 259–273. (b) Zhang, S. S.; Nie, S. P.; Huang, D. F.; Huang, J. Q.; Wang, Y. W.; Xie, M. Y. *J. Agric. Food Chem.* **2013**, *61*, 3637–3682. (c) Ma, B. J.; Ren, W.; Zhou, Y.; Ma, J. C.; Ruan, Y.; Wen, C. N. N. *Am. J. Med. S.* **2011**, *3*, 495–498. (d) Wu, G. S.; Bao, J. L.; Li, X. W.; Chen, X. P.; Lu, J. J.; Wang, Y. T. *Expert Opin. Inv. Drugs* **2013**, *22*, 981–992.

(3) (a) Niu, X. M.; Qiu, M. H.; Li, Z. R.; Lu, Y.; Cao, P.; Zheng, Q. T. *Tetrahedron Lett.* **2004**, *45*, 2989–2993. (b) Wang, C. F.; Liu, J. Q.; Yan, Y. X.; Chen, J. C.; Lu, Y.; Guo, Y. H.; Qiu, M. H. *Org. Lett.* **2010**, *12*, 1656–1659. (c) Liu, J. Q.; Wang, C. F.; Li, Y.; Luo, H. R.; Qiu, M. H. *Planta Med.* **2012**, *78*, 368–376.

(4) (a) Peng, X. R.; Liu, J. Q.; Xia, J. J.; Yang, Y. H.; Qiu, M. H. *Chin. Trad. Herb. Drugs* **2012**, *43*, 1045–1049. (b) Peng, X. R.; Liu, J. Q.; Wang, C. F.; Li, X. Y.; Shu, Y.; Zhou, L.; Qiu, M. H. *J. Nat. Prod.* **2014**, *77*, 737–743.

(5) Mothana, R. A. A.; Jansen, R.; Julich, W. D.; Lindequist, U. *J. Nat. Prod.* **2000**, *63*, 416–418.

(6) Niu, X. M.; Li, S. H.; Sun, H. D.; Che, C. T. *J. Nat. Prod.* **2006**, *69*, 1364–1365.

(7) Dine, R. S. E.; Halawany, A. M. E.; Ma, C. M.; Hattori, M. *J. Nat. Prod.* **2009**, *72*, 2019–2023.

(8) Yan, Y. M.; Ai, J.; Zhou, L. L.; Chung, A. C. K.; Li, R.; Nie, J.; Fang, P. F.; Wang, X. L.; Luo, J.; Hu, Q.; Hou, F. F.; Cheng, Y. X. *Org. Lett.* **2013**, *15*, 5488–5491.

(9) Williams, P.; Sorribas, A.; Howes, M. J. R. *Nat. Prod. Rep.* **2011**, *28*, 48–77.

(10) (a) Bartus, R. T.; Dean, R. L.; Pontecorvo, M. J.; Flicker, C. *Ann. N.Y. Acad. Sci.* **1985**, *444*, 332–358. (b) Ruberg, M.; Rieger, F.; Villageois, A.; Bonnet, A. M.; Agid, Y. *Brain Res.* **1986**, *362*, 83–91.

(11) (a) Zhang, Y.; Luo, J.; Huang, N. H.; Zhang, X. Y. *Chin. J. Exptal. Trad. Med.* **2012**, *18*, 172–175. (b) Song, M. J.; Sun, W. W.; Bao, H. Y. *Mycosystema* **2012**, *31*, 762–768.

(12) (a) Howes, M. R.; Houghton, P. J. *Pharmacol., Biochem. Behav.* **2003**, *75*, 513–527. (b) Kumar, P.; Singh, V. K.; Singh, D. K. *Phytother. Res.* **2009**, *23*, 172–177.

(13) Houk, K. N.; Luskus, L. J. *J. Am. Chem. Soc.* **1971**, *93*, 4606–4607.